Anal. Chem. **2008,** *80,* 4689–4695

Determining Subnanomolar Iron Concentrations in Oceanic Seawater Using a Siderophore-Modified Film Analyzed by Infrared Spectroscopy

Eric G. Roy,[†,‡] Cuihong Jiang,[‡,§] Mark L. Wells,[†] and Carl Tripp*[,‡,§]

School of Marine Sciences, Laboratory for Surface Science and Technology, and Department of Chemistry, University of Maine, Orono, Maine 04469

Iron is a bioactive trace element in seawater that regulates photosynthetic carbon dioxide drawdown and export from surface waters by phytoplankton in upward of 40% of the world's oceans. While autonomous sensor arrays are beginning to provide high-resolution data on temporal and spatial scales for some key oceanographic parameters, current analytical methods for iron are not amenable to autonomous platforms because of the need for user involvement and wet chemistry-based approaches. As a result, very large gaps remain in our understanding of iron distribution and chemistry in seawater. Here we present a straightforward nanostructure-based method to measure dissolved iron in natural seawater. The device comprises an iron-specific chelating biomolecule, desferrioxamine B (DFB), covalently immobilized on a mesoporous silica film. Changes in infrared spectral signatures of the immobilized DFB upon Fe(III) complexation provide an accurate and precise measure of iron on the surface of a chip exposed to seawater. The current system has a detection limit of ~50 pM for a 1-L sample at pH 1.7 and was used to measure dissolved iron in subarctic Pacific waters without interference from other elements in seawater. This technology provides a major step toward obtaining accurate iron measurements on autonomous research platforms.

In upward of 40% of the world's ocean, photosynthetic drawdown of carbon dioxide is limited by the availability of dissolved iron in surface waters.[1–3] The marine biogeochemistry of iron therefore has significant implications for regulating carbon dioxide flux at the air/sea interface and thus climate change. Although iron limitation in subarctic Pacific, equatorial Pacific, and Southern Ocean surface waters now is well demonstrated, the paucity of field data on the distributions of iron and other bioactive metals makes it difficult to fully quantify their effects on the global carbon cycle. Recently, autonomous gliders, depth profilers, and mooring networks have been outfitted with a range of sensors to reverse oceanographic data shortage, but there are no deployable iron sensors that can measure iron at the (sub)nanomolar levels found in most ocean waters, due in large part to the analytical difficulties associated with their development.

Measuring iron in seawater is extremely challenging. Due to a combination of the low solubility of iron in oxic seawater and the comparatively high iron demand by phytoplankton, iron concentrations in oceanic surface waters can be extremely low ($\ll$1 nM). As a consequence, it is easy to contaminate samples during both the sampling and the analytical processes. The chemical speciation of iron in the ocean also complicates the analytical process. The majority of the ambient dissolved iron(III) (<99%) in seawater resides in strong but unidentified organic complexes at equilibrium.[4,5] In addition to these soluble iron(III) species, significant fractions of "dissolved" iron (<0.4 μm) in ocean waters can reside in colloidal matter,[6,7] likely mainly as organic complexes[8,9] as well as in reduced iron(II) species in the upper photic zone.[10–12] As a consequence, seawater samples are acidified to pH $\leq$ 1.8 for 12 h to minimize these complicating factors on the determinations of total dissolved iron.[13]

* To whom correspondence should be addressed. E-mail: ctripp@maine.edu.
† School of Marine Sciences.
‡ Laboratory for Surface Science and Technology.
§ Department of Chemistry.

(1) Martin, J. H.; Fitzwater, S. E. *Nature* **1988**, *331*, 341–343.
(2) Tsuda, A.; Takeda, S.; Saito, H.; Nishioka, J.; Nojiri, Y.; Kudo, I.; Kiyosawa, H.; Shiomoto, A.; Imai, K.; Ono, T.; Shimamoto, A.; Tsumune, D.; Yoshimura, T.; Aono, T.; Hinuma, A.; Kinugasa, M.; Suzuki, K.; Sohrin, Y.; Noiri, Y.; Tani, H.; Deguchi, Y.; Tsurushima, N.; Ogawa, H.; Fukami, K.; Kuma, K.; Saino, T. *Science* **2003**, *300*, 958–961.
(3) Coale, K. H.; Johnson, K. S.; Chavez, F. P.; Buesseler, K. O.; Barber, R. T.; Brzezinski, M. A.; Cochlan, W. P.; Millero, F. J.; Falkowski, P. G.; Bauer, J. E.; Wanninkhof, R. H.; Kudela, R. M.; Altabet, M. A.; Hales, B. E.; Takahashi, T.; Landry, M. R.; Bidigare, R. R.; Wang, X.; Chase, Z.; Strutton, P. G.; Friederich, G. E.; Gorbunov, M. Y.; Lance, V. P.; Hilting, A. K.; Hiscock, M. R.; Demarest, M.; Hiscock, W. T.; Sullivan, K. F.; Tanner, S. J.; Gordon, R. M.; Hunter, C. N.; Elrod, V. A.; Fitzwater, S. E.; Jones, J. L.; Tozzi, S.; Koblizek, M.; Roberts, A. E.; Herndon, J.; Brewster, J.; Ladizinsky, N.; Smith, G.; Cooper, D.; Timothy, D.; Brown, S. L.; Selph, K. E.; Sheridan, C. C.; Twining, B. S.; Johnson, Z. I. *Science* **2004**, *304*, 408–414.
(4) Gledhill, M.; Van den Berg, C. M. G. *Mar. Chem.* **1994**, *47*, 41–54.
(5) Rue, E. L.; Bruland, K. W. *Mar. Chem.* **1995**, *50*, 117–138.
(6) Wells, M. L.; Mayer, L. M.; Donard, O. F. X.; De Souza Sierra, M. M.; Ackelson, S. G. *Nature* **1991**, *353*, 248–250.
(7) Bergquist, B. A.; Wu, J.; Boyle, E. A. *Geochim. Cosmochim. Acta* **2007**, *71*, 2960–2974.
(8) Cullen, J. T.; Bergquist, B. A.; Moffett, J. W. *Mar. Chem.* **2006**, *98*, 295–303.
(9) Wells, M. L. *Biogeochem. Mar. Dissolved Org. Matter* **2002**, 367–404.
(10) Roy, E. G.; Wells, M. L.; King, D. W. *Limnol. Oceanogr.* **2008**, *53*, 89–98.
(11) Kuma, K.; Nakabayashi, S.; Matsunaga, K. *Water Res.* **1995**, *29*, 1559–1569.
(12) Ussher, S. J.; Worsfold, P. J.; Achterberg, E. P.; Laes, A.; Blain, S.; Laan, P.; de Baar, H. J. W. *Limnol. Oceanogr.* **2007**, *52*, 2530–2539.
(13) Cutter, G.; Andersson, P.; Codispoti, L.; Croot, P. L.; Francois, R.; Lohan, M. C.; Obata, H.; van der Loeff, M. http://www.ldeo.columbia.edu/res/pi/geotraces/documents/GEOTRACESIPYProtocols-Final.pdf, 2007.

10.1021/ac800356p CCC: $40.75 © 2008 American Chemical Society
Published on Web 05/22/2008

Marine iron determinations are further complicated by the seawater matrix, which contains ~3% salt and a range of other elements that can potentially interfere with trace metal analysis. For the most reliable analytical methods (e.g., inductively coupled plasma mass spectrometry (ICPMS) and graphite furnace atomic absorption (GF-AA)), these salts must first be separated from the trace metals using, for example, a chelating resin prior to elution to the downstream instrument.[14] Moreover, ICPMS and GF-AA are laboratory-based methods and, therefore, cannot provide marine researchers with continuous measurements while at sea. Over the past 15 years, colorimetric and chemiluminescent techniques have been developed to measure iron on shipboard platforms,[15–17] but these methods require rigorous sample treatment and a high level of user interaction and expertise, thereby limiting their routine application. A number of these analytical methods have been adapted for in situ deployment in some oceanographic regimes,[18–21] but the detection limits of these in situ methods are not low enough for routine deployment in HNLC waters. In addition to these techniques, promising fluorescence-based detection systems have been reported for detecting dissolved iron in aqueous media.[22,23] These systems measure the most chemically labile iron species at circumneutral pH, and reported limits are such that they could potentially measure iron in HNLC waters. While these methods represent a significant step forward in analytical capabilities by measuring iron at circumneutral pH, they are unable to detect iron in acidified samples and thus measurements cannot be compared directly with historical data sets or samples collected and analyzed using currently recommended sample treatment protocols.[13]

We set out to improve on this earlier work by developing a nanostructure-based, biomimetic iron detection technique that is functional over a wide range of pH and capable of measuring iron at the <100 pM Fe concentrations found in many oceanic surface waters. Our approach utilizes disposable chips bearing a mesoporous oxide surface modified by attaching an iron-selective molecule that can be probed for analysis by infrared spectroscopy. To identify an iron-specific complexing molecule we turned to biology, where many heterotrophic bacteria release low molecular weight, iron-specific chelators termed siderophores to facilitate iron acquisition. DFB, a commercially available siderophore produced by *Streptomyces pilosus* and other prokaryotes, is a linear molecule consisting of three repeating hydroxamate subunits and an amine tail (Figure 1A). The chelate molecule, Fe(III)−DFB, consists of two closed loops that coordinate iron in a hexadentate fashion (Figure 1B). DFB has a very high affinity and selectivity for iron.[24,25] Typical thermodynamic constants for Fe−DFB are on the order of 10^{32}, roughly 15 orders in magnitude higher than the closest competing metal at marine pH, Cu(II).[25] Tests in seawater, where the side reactions of both DFB and Fe(III) yield a conditional stability for Fe′ (the sum of inorganic Fe(III) species) of $K^{cond}_{L,Fe(III)'} \cong 10^{16.5}$,[5,26,27] show that DFB can be used to manipulate iron availability in phytoplankton incubation experiments by acquiring iron from the ambient complexing molecules in seawater,[28–31] which have conditional stability constants for Fe′ that are 3−4 orders of magnitude lower.[5,26,27] Given DFB's chemical selectivity for iron in seawater,[5] it provides an ideal starting point for engineering a nanostructure-based, biomimetic sensor for iron.

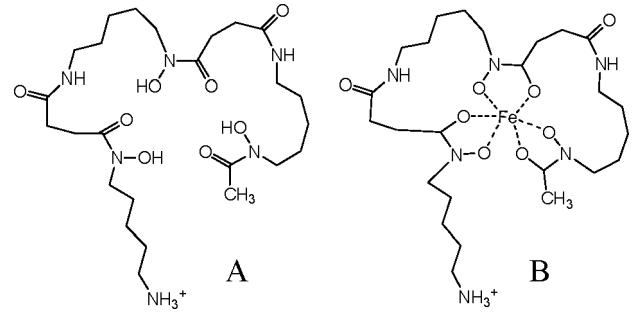

Figure 1. Structure of (A) desferrioxamine B (DFB) and (B) ferrioxamine B (Fe-DFB).

Our detection system utilizes Fourier transform infrared spectroscopy (FT-IR) because it is a powerful tool for acquiring molecular structure information. A detailed FT-IR study of DFB powder shows that clear and identifiable spectral changes occur upon iron chelation.[32] Infrared spectroscopy also has been used to study spectral features of different metals chelated by hydroxamate ligands.[33,34] Because unique IR spectra are obtained for each metal chelated, an IR-based detection system provides an added potential level of analytical selectivity in developing metal sensors for complex solutions like seawater.

In our approach, the DFB is anchored to a silicon wafer coated by a mesoporous silica coating. Mesoporous silicas are used in a number of sensing applications because they are easily prepared by sol−gel routes and applied to surfaces as thin films.[35,36] These

(14) Lohan, M. C.; Aguilar-Islas, A. M.; Franks, R. P.; Bruland, K. W. *Anal. Chim. Acta* **2005**, *530*, 121–129.
(15) King, D. W.; Lounsbury, H. A.; Millero, F. J. *Environ. Sci. Technol.* **1995**, *29*, 818–824.
(16) Lohan, M. C.; Aguilar-Islas, A. M.; Bruland, K. W. *Limnol. Oceanogr.: Methods* **2006**, *4*, 164–171.
(17) Measures, C. I.; Yuan, J.; Resing, J. A. *Mar. Chem.* **1995**, *50*, 3–12.
(18) Coale, K. H.; Chin, C. S.; Massoth, G. J.; Johnson, K. S.; Baker, E. T. *Nature (London, United Kingdom)* **1991**, *352*, 325–328.
(19) Chapin, T. P.; Jannasch, H. W.; Johnson, K. S. *Anal. Chim. Acta* **2002**, *463*, 265–274.
(20) Laes, A.; Vuillemin, R.; Leilde, B.; Sarthou, G.; Bournot-Marec, C.; Blain, S. *Mar. Chem.* **2005**, *97*, 347–356.
(21) Luther, G. W.III.; Brendel, P. J.; Lewis, B. L.; Sundby, B.; Lefrancois, L.; Silverberg, N.; Nuzzio, D. B. *Limnol. Oceanogr.* **1998**, *43*, 325–333.
(22) Lam, C. K. S. C. C.; Jickells, T. D.; Richardson, D. J.; Russell, D. A. *Anal. Chem.* **2006**, *78*, 5040–5045.
(23) Barrero, J. M.; Camara, C.; Perez-Conde, M. C.; San Jose, C.; Fernandez, L. *Analyst* **1995**, *120*, 431–435.
(24) Hernlem, B. J.; Vane, L. M.; Sayles, G. D. *Inorg. Chim. Acta* **1996**, *244*, 179–184.
(25) Martel, A. E.; Smith, R. M. *Critical Stability Constants*; Plenum Press: New York, 1982.
(26) Buck, K. N.; Bruland, K. W. *Limnol. Oceanogr.* **2007**, *52*, 1800–1808.
(27) Witter, A. E.; Hutchins, D. A.; Butler, A.; Luther, G. W. *Mar. Chem.* **2000**, *69*, 1–17.
(28) Wells, M. L.; Trick, C. G. *Mar. Chem.* **2004**, *86*, 1–13.
(29) Granger, J.; Price, N. M. *Limnol. Oceanogr.* **1999**, *44*, 541–555.
(30) Wells, M. L. *Limnol. Oceanogr.* **1999**, *44*, 1002–1008.
(31) Wells, M. L.; Price, N. M.; Bruland, K. W. *Limnol. Oceanogr.* **1994**, *39*, 1481–1486.
(32) Cozar, O.; Leopold, N.; Jelic, C.; Chis, V.; David, L.; Mocanu, A.; el Tomoaia-Cotis, M. *J. Mol. Struct.* **2006**, *788*, 1–6.
(33) Brown, D. A.; McKeith, D.; Glass, W. K. *Inorg. Chim. Acta* **1979**, *35*, 57–60.
(34) Bhatt, K.; Agrawal, Y. K. *Synth. Inorg. Met.-Org. Chem.* **1972**, *2*, 175–179.
(35) Anderson, M. T.; Martin, J. E.; Odinek, J. G.; Newcomer, P. *Mater. Res. Soc. Symp. Proc.* **1996**, *431*, 217–223.
(36) Lu, Y.; Han, L.; Brinker, C. J.; Niemczyk, T. M.; Lopez, G. P. *Sens. Actuators, B: Chem. Proc. 1996 6th Int. Meet. Chem. Sens. Part 2* **1996**, *B36*, 517–521.

materials can be fabricated with high surface areas (~1500 m^2/g[37]) that can be modified with silanes to facilitate immobilization of biomolecules.[38] Mesoporous silica is an ideal substrate here because it is transparent in the IR regions critical for evaluating DFB surface attachment chemistry, as well as for measuring spectral changes in DFB upon iron chelation.

In this work, we report the successful development of a biomimetic chip-based analytical system for measuring dissolved iron in seawater. Selectivity for iron comes from the surface attachment of the iron-selective molecule (DFB) to a mesoporous silica film. The transduction mechanism of this device is an infrared spectral change upon exposure to samples containing iron. The high information content intrinsic to FT-IR analysis adds confidence in the method's selective detection of iron. This approach is similar to traditional solid-phase extraction; iron is concentrated on a substrate; however, the chip-based method measures iron directly on the substrate rather than after elution to a downstream instrument, thereby greatly simplifying the measurement process and minimizing the potential for sample contamination. The DFB chip-based system was tested in a shipboard laboratory to accurately measure iron in certified and field seawater samples (pH 1.7−8.0) in the subarctic Pacific. The device performed without interference from other metals or the seawater matrix and provided precise and accurate iron determinations even at the ultralow (<100 pM) concentrations in these oceanic surface waters.

MATERIALS AND METHODS

Reagents. All reagents were of best commercially available purity and were used as received, unless otherwise noted. Toluene, DFB, 1-ethyl-3-(3-dimethylaminopropyl) carbodiimide hydrochloride (EDC), cetyltrimethalammonium bromide (CTAB), oxalic acid, hydrogen peroxide, methanol, and Fe(III) atomic absorption standard were purchased from Fisher Scientific. Ethanol, tetraethylorthosilicate (TEOS), ethylene diamine (EDA), and 2-(*N*-morpholino)ethanesulfonic acid (MES) were purchased from Sigma Aldrich, and 3-(triethoxysilyl)propylsuccinic anhydride (anhydride silane) was purchased from Gelest. Deionized water (resistivity >18.1 MU cm) was used throughout.

Sol−Gel Synthesis. An MCM-48 sol was prepared by combining 1.25 g of water, 10.35 g of ethanol, 0.125 mL of 0.03 M HCl, and 16.4 mL of TEOS in an acid-washed flask.[37] The mixture was stirred and refluxed at 60 °C for 2 h. Ten milliliters of sol then was added to 20.17 g of ethanol, 0.1 mL of 1 M HCl, 1.75 g of water, and 1.3 g of CTAB to template a cubic 3D sol−gel. This solution was aged in a covered Erlenmeyer flask for 1 week at room temperature prior to use.

Preparation of Sol−Gel Coated Wafer. A 4-in.-diameter silicon wafer 2 mm thick was used as an inexpensive, infrared transparent substrate for the DFB-based sensor. The 2-mm thickness minimized spectral fringing, and the wafer was doubly polished to prevent optical scattering. Both sides of the wafer were irradiated with UV light (254 nM) for 45 min and exposed to 30% H_2O_2 for 10 min to generate an organic-free oxide layer. After the initial cleaning, the wafer was immediately placed in a spin coater and securely held in place by vacuum. The surface of the wafer then was rinsed with methanol and spun dry. Once dry, ~ 5 mL of the aged sol−gel was added dropwise to the surface and the wafer then spun at 3000 rpm for 45 s. The silicon wafer coated with the sol−gel film was then calcined in a baffle furnace at a temperature ramp rate of 1 °C/min from 22 to 450 °C for 3 h. The coating procedure was repeated on the other side of the wafer. This procedure produces a homogeneous, high surface area (~1500 m^2/g) mesoporous film[37] to serve as a scaffold for DFB attachment.

Surface Attachment of DFB to Mesoporous Silica Surface. DFB was attached to the mesoporous silica film through an anhydride silane linker molecule. The silica-coated wafer was modified to contain anhydride groups through a base-catalyzed reaction between an anhydride silane and the isolated silanol groups on silica[39] by immersing the wafer in 100 mL of toluene containing 2 mL of EDA and stirring for 10 min at room temperature. The wafer was rinsed with 25 mL of toluene and immersed in a stirring solution of 100 mL of toluene and 2 mL of anhydride silane for 1 h under nitrogen at room temperature. The anhydride-modified wafer was thoroughly rinsed with toluene, dried under N_2, and immersed in water for 15 min to convert the anhydride group to carboxylic acid groups that can form an amide bond with the amine tail of DFB.[40] To form this amide linkage, 1.5 g of Fe(III)−DFB and 1.0 g of EDC were dissolved in 100 mL of 0.01 M MES buffer (pH 5.0) and reacted with the wafer for 3 h at room temperature while stirring. We found that the amide coupling of DFB to the surface was more efficient when DFB was preloaded with iron. The DFB-modified wafer was thoroughly rinsed with deionized water and dried under N_2. The wafer was scored into a 9.2 mm × 9.2 mm grid, using an automated chip dicer, immersed in 0.01 M Optima grade HCl overnight to remove metal contaminants, and then immersed in a 10 mM solution of oxalic acid (pH 3.0) for 2 h, to remove iron from DFB through ligand exchange.[41] Prior to storage at 4 °C, the wafer was rinsed with deionized water and dried with N_2. Individual chips were easily broken from the scored wafer as needed using acid-cleaned polypropylene forceps.

FT-IR Spectroscopy. Transmission FT-IR was used to monitor the surface reactions during DFB attachment to the mesoporous silica-coated chip, as well as for iron quantification. All spectra are reported as difference spectra, using a silica-coated silicon wafer as a reference, unless otherwise noted. In these spectra, positive bands are from bonds formed on the chip, and negative bands are from removed bonds. All spectra were collected on a N_2-purged Bomem FT-IR spectrometer, equipped with a liquid N_2-cooled MCT detector. A custom-fabricated Teflon vessel securely held the chips in the 12-mm-diameter infrared beam without exposing them to contaminating metal surfaces. Typically, 100 scans were coadded at 8 cm^{-1} resolution and each spectrum required ~1 min of scan time. All baseline corrections and other signal processing were carried out using the Thermo Galactic GRAMS AI software that accompanies the instrument with the PLSplus/IQ package.

Quantification of Fe(III) on the Chip. Complexation of Fe(III) by the immobilized DFB on the chip surface was

(37) McCool, B.; Murphy, L.; Tripp, C. P. *J. Colloid Interface Sci.* **2006**, *295*, 294–298.
(38) Slowing, I. I.; Trewyn, B. G.; Giri, S.; Lin, V. S. Y. *Adv. Funct. Mater.* **2007**, *17*, 1225–1236.
(39) Kanan, S. M.; Tze, W. T. Y.; Tripp, C. P. *Langmuir* **2002**, *18*, 6623.
(40) Grabarek, Z.; Gergely, J. *Anal. Biochem.* **1990**, *185*, 131–135.
(41) Kunkely, H.; Vogler, A. *Inorg. Chem. Commun.* **2001**, *4*, 215–217.

determined by IR spectroscopy. In brief, the integrated intensity of the Fe−O band at 560 cm^{-1} (valley-to-valley baseline corrected with integration limits of 528.9−590.8 cm^{-1}) was used for Fe(III) quantification because this band showed little interference from the sample matrix (see Results and Discussion). The extinction coefficient of the integrated intensity of the 560-cm^{-1} band was determined from Beer−Lambert plots generated using known amounts of Fe−DFB dispersed on a PTFE window. Specifically, a 7.0×10^{-4} M Fe−DFB solution was prepared in methanol, and known volumes (multiples of 100-μL aliquots) of the solution was dispersed evenly on the window of a 13-mm-diameter porous PTFE IR sample card (International Crystal Laboratories). Once the solvent had dried fully (~30 min), the absorbance spectrum was recorded as described above using an unexposed PTFE window as a reference. Based on five repetitions of this calibration procedure, the extinction coefficient of the integrated intensity of the 560-cm^{-1} band was 5.1×10^4 ($\pm -8.2 \times 10^2$) g Fe−DFB^{-1} cm^2.

Chip Exposure to Iron Solutions and Possible Ion Interferences in Seawater. To minimize iron contamination during sampling and analysis, the chips always were handled under HEPA-purified air using trace metal clean procedures.[42] Before exposing the chips to seawater samples or standards, they first were wetted by rinsing with deionized water. The chips were exposed to samples and standards by suspension in 1 L of stirring solution for 8 h. Given the high conditional constant of the Fe(III)−DFB complex, iron accumulation on the chip is controlled by the mass transport kinetics of reactive iron to the chip surface. Due to the rudimentary fluidics control in these batch experiments, we found empirically that 8 h of stirring was sufficient to fully extract dissolved iron from the 1-L seawater samples (amended $[Fe(III)_0 = 1$ and 10 nM). Periodic measurements by chemiluminescent flow injection analysis (FIA-CL) (determined by reduction of Fe(III) to Fe(II) followed by detection by oxidative luminol chemiluminescence[43]) confirmed that no residual iron in the acidified (pH 1.7) seawater after 8 h, indicating that all dissolved iron was delivered to the chip surface under our conditions.

Following exposure to the solution, the chips were rinsed with DI water and dried with N_2. At this time, IR spectra were collected using the same parameters as described above. The total mass of iron sequestered to the biomimetic surface was calculated from the measured integrated intensity of the Fe−O peak at 560 cm^{-1} and the physical area of the sample chip (1.69 cm^2). Knowledge of the sample volume leads directly to a value for the dissolved iron concentration.

The possible interferences from other metal cations in the seawater matrix were investigated by exposing the chips to oxic solutions (pH 2.0) of elements in seawater (Na, Mg, Ca, Al, Cr, Mn, Co, Ni, Cu, Zn) at or above typical seawater concentrations. Solutions containing Na, Mg, and Ca first were passed through a column packed with Toyopearl AF Chelate 650 M to minimize trace metal contaminants. The exposure procedure described above for iron determination was used for each solution used to test for interferences.

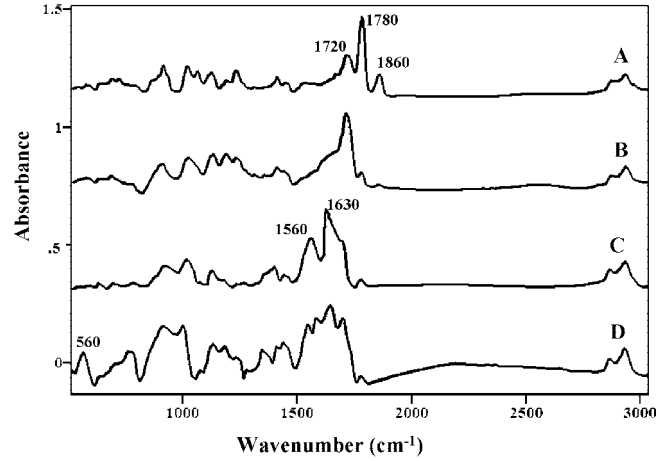

Figure 2. FT-IR difference spectra for each of the synthetic steps during DFB modification of the silicon substrate. (A) Anhydride silane modification; (B) carboxylic acid modification; (C) DFB modification; (D) Fe(III) addition. All spectra are recorded as difference spectra, using an unmodified silica-coated chip as a reference. For clarity, all spectra are artificially offset and have been baseline corrected to yield a level baseline.

Table 1. Comparison of Certified Iron Values in Acidified Seawater Samples (pH 1.7) Measured by DFB Chip-Based Detection System[a]

sample	[Fe] accepted (nM)	[Fe] measured (nM)
NASS-5	3.71 ± 0.63	3.65 ± 0.14
SAFe D2	0.91	1.08 ± 0.10
SAFe S1	0.091	0.102 ± 0.012

[a] NASS-5 is North Atlantic Surface Seawater and the SAFe samples were obtained from UCSC (requestsafestandard@UCSC.edu).

Field Sample Collection. Field samples were collected during an oceanographic research cruise to Ocean Station PAPA (50°N, 145° W) in the subarctic Pacific during May 2007. Samples were collected to a depth of 800 m using a 5-L Teflon-coated Go-Flo bottle (General Oceanics) that was suspended on a Kevlar line and tripped using a Teflon messenger. Upon returning to the surface, the Go-Flo bottle was transferred into the shipboard clean room and pressurized with N_2. The water was filtered through a 0.45-μm acid-cleaned Teflon cartridge filter (Sterlitech). Each filtered sample was collected in three acid-cleaned FPE bottles (Nalgene) and acidified to pH 1.7 with Optima grade HCl (Fisher Scientific) for 24 h before analysis. Two of the three samples were exposed to the chips after short-term acidification (24 h), and a number of subsamples were transferred into a foil-wrapped Teflon bottle for UV oxidation. A mercury pen lamp (Ultraviolet Products), protected by an acid-cleaned quartz tube, was lowered into the sample for 24 h to UV destroy dissolved organic matter (DOM) in selected natural samples.

RESULTS AND DISCUSSION

Surface Attachment of DFB to Mesoporous Silica Film. Infrared spectroscopy was used to monitor the synthetic steps during DFB surface attachment (Figure 2). Figure 2A shows the spectrum of the anhydride silane modified chip, using a silica-coated chip as a reference. Positive bands at 1860 and 1780 cm^{-1} are attributed to anhydride carbonyl stretching modes, and the

(42) Bruland, K. W.; Franks, R. P.; Knauer, G. A.; Martin, J. H. *Anal. Chim. Acta* **1979**, *105*, 233–245.
(43) Lannuzel, D.; de Jong, J.; Schoemann, V.; Trevena, A.; Tison, J.-L.; Chou, L. *Anal. Chim. Acta* **2006**, *556*, 476–483.

Table 2. Repeated Measurements of 0.50 nM Seawater Samples Using Sequentially Regenerated Surfaces of DFB Modified Chips

cycle	[Fe] (nM) ± 1 SD
1	0.51 ± 0.02
2	0.44 ± 0.01
3	0.49 ± 0.02
4	0.50 ± 0.03
5	0.47 ± 0.02
6	0.49 ± 0.02
7	0.46 ± 0.03
8	0.47 ± 0.02
9	0.48 ± 0.01
10	0.49 ± 0.03

1720-cm^{-1} peak is due to the C=O stretching mode of a carboxylic acid arising from the hydrolysis of the anhydride ring to the acid by residual water. A negative band at 3747 cm^{-1} (not shown) is due to the disappearance of silanol groups on the silica surface after silane attachment to the silica surface. The solution-phase reaction yielded up to a 500-fold surface coverage enhancement of anhydride silane, compared to the same reaction in the vapor phase (data not shown). The increase in coverage in solution-phase synthesis is due to surface polymerization of anhydride silane, catalyzed by trace amounts of water.[45] Figure 2B shows the spectrum after the anhydride ring has been hydrolyzed by submerging the wafer in water. The bands at 1860 and 1780 cm^{-1} are reduced by 90%, and the large band that forms at 1720 cm^{-1} is due to the newly formed carboxylic acids.

The IR spectrum after attachment of DFB to the surface followed by Fe(III) removal by oxalic acid is shown in Figure 2C. Strong amide peaks around 1630 and 1560 cm^{-1} appear in the spectrum, showing that the carboxylic acid group of the silane reacted to form amide linkages with the amine tail of Fe(III)−DFB. However, a shoulder still remains at 1720 cm^{-1} showing that a small fraction (7−12%) of the carboxylic acid groups are inaccessible to the amine coupling reaction (Figure 2C). Complexation of iron by the immobilized DFB causes a significant shift in the IR spectrum whereby the large amide I peak at 1630 cm^{-1} shifts to 1645 cm^{-1} and the amide (II) peak at 1560 cm^{-1} shifts to 1570 cm^{-1} (Figure 2D). These spectral shifts are in agreement with IR spectra obtained in the solution phase reaction of Fe(III) with DFB.[32] Another notable feature of Figure 2D is a strong peak found at 560 cm^{-1}, assigned by others to a Fe−O stretching mode.[32] This assignment is verified in this work. This band shifts in frequency to varying degress when the immobilized DFB is exposed to solutions containing other metal cations (see Table 3).

Selection of the 560-cm^{-1} Band for Quantification of Fe(III). Clearly, there are several differences between the IR spectra of immobilized DFB and immobilized Fe−DFB that potentially could be used to detect and quantify Fe in aqueous solutions. However, we find that shifts in frequency and shape for a majority of the bands are sensitive to the solution matrix. The difference spectra (500−1800 cm^{-1}) of three separate chips after exposure to 50 mL of 200 nM Fe(III) solution prepared in deionized water, UV-oxidized (organic matter-free) seawater, or

(44) Silberzan, P.; Leger, L.; Ausserre, D.; Benattar, J. J. *Langmuir* **1991**, *7*, 1647–1651.

(45) Tripp, C. P.; Hair, M. L. *Langmuir* **1995**, *11*, 1215–1219.

Table 3. Elements Tested for Possible Interference of DFB Chip-Based Sensor at Levels up to 10 Times Higher than Concentrations Found in Seawater[a]

element	typical seawater concentration (M)[b]	tested concentration (M)	M-O stretching mode (cm^{-1})
Na^{+}	0.47	1	nd
Mg^{2+}	5×10^{-2}	5×10^{-2}	nd
Ca^{2+}	1×10^{-2}	1×10^{-2}	nd
Al^{3+}	1×10^{-8}	1×10^{-7}	nd
Cr	4×10^{-9}	1×10^{-8}	nd
Mn^{2+}	5×10^{-10}	1×10^{-9}	608
Fe^{2+}	varies	1×10^{-9}	560
Co^{2+}	2×10^{-11}	1×10^{-10}	604
Ni^{2+}	8×10^{-9}	1×10^{-8}	629
Cu^{2+}	4×10^{-9}	1×10^{-8}	610
Zn^{2+}	6×10^{-9}	1×10^{-8}	633

[a] The wavenumbers of detectable peaks are shown. [b] From ref 51.

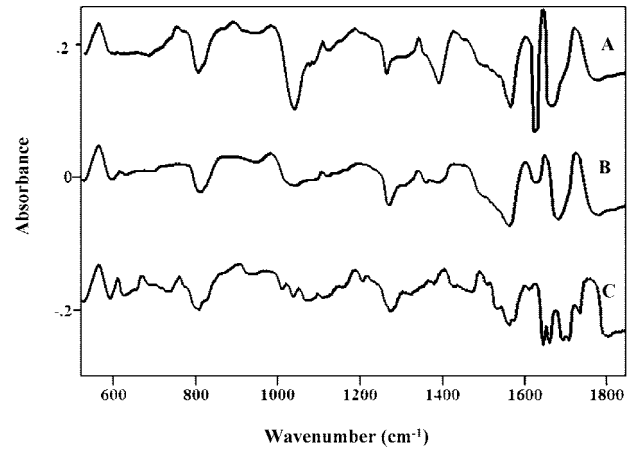

Figure 3. Difference spectra after iron saturation of the chip: (A) in freshwater; (B) in UV oxidized seawater, and (C) in natural seawater, using an iron-free DFB-immobilized chip as a reference. For clarity, all spectra are offset and have been baseline corrected to yield a level baseline.

natural seawater are shown in Figure 3. Using the DFB modified chip as a reference illustrates the subtle changes in peak position and shape that are amplified in the difference spectrum. For example, the spectral distortion in the amide region (1550−1670 cm^{-1}) is not consistent among samples and therefore could not be incorporated into a chemometric analysis for iron measurements. Additional bands appear in the difference spectrum between 600 and 1800 cm^{-1} after the chips are exposed to natural seawater (Figure 3C). These peaks do not appear in subsamples that have been UV oxidized, suggesting that they mainly result from the sorption of naturally occurring DOM in seawater. The intensity of these purported DOM bands also varied significantly among natural samples collected from different depths.

An identical Fe−O peak at 560 cm^{-1}, well removed from DOM interferents, was insensitive to water matrix and the DOM peaks did not overlay with this band. We used the integrated area of this single peak to measure the concentration of Fe(III) in seawater. Standard additions (triplicate analyses for each standard) were performed in low-iron seawater (1-L volume) to determine the system response in a saline matrix (Figure 4), at three pH values (1.7, 4.5, 8.0). The curves were linear from 0 to 10 nM Fe(III), and the theoretical detection limit (defined as 3 SD of

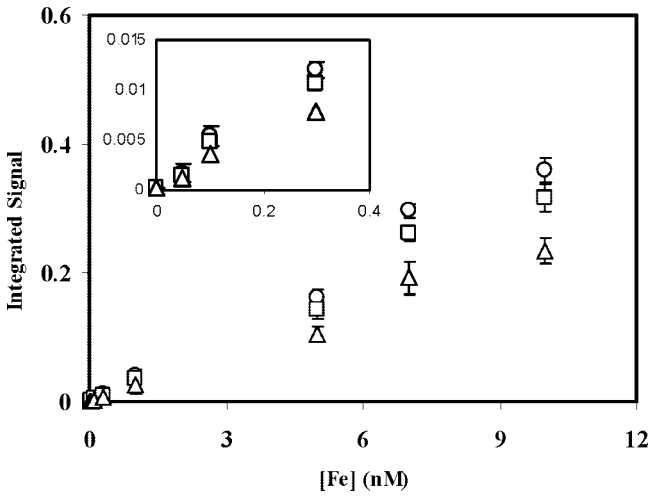

Figure 4. Calibration curves for 1L seawater samples at pH 1.7 (circles), 4.5 (squares), and 8.0 (triangles). Inset shows standards between 0 and 0.3 nM in more detail. Error bars represent ±1 standard deviation of replicate ($n = 3$) measurements.

blank replicates) was 48 pM for 1-L seawater samples at pH 1.7, 55 pM for 1-L seawater sample at pH 4.5, and 59 pM for 1-L seawater sample at pH 8.0. Equations for linear fits are listed in Supporting Information, as well as difference spectra showing the 560 cm^{-1} peak for 50, 100, and 300 pM standards made in 1 L of natural seawater (pH 1.7). Iron concentrations were successfully measured at all depths, with the lowest values determined in the 1-L field samples being 78 pM at pH 1.7, 97 pM at pH 4.5, and 88 pM at pH 8.0. FIA-CL analysis of the iron remaining in the pH 1.7 seawater samples after the 8-h exposure verified that the DFB immobilized chips recovered 98 ± 4% of total dissolved iron. The accuracy of the DFB-based sensor, determined using different certified seawater samples at pH 1.7, was within 10% of accepted values (Table 1).

Iron recoveries by the chips decreased progressively with increasing pH (Figure 4). This decrease did not result from interference in the IR spectra but appeared instead to be related to changes in the ambient iron chemistry affecting either the reaction kinetics or perhaps the inherent extent of iron exchange between "dissolved" species and immobilized DFB. It is well recognized that the pH-dependent increase in complexation abilities of natural ligands leads to interference in iron-exchange kinetics.[16] Alternatively, it is possible that colloidal forms of iron found in seawater[7] are more prevalent at higher pH, though much of this colloidal iron may exist as organic complexes instead of mineral forms.[9] While calibration slopes decreased by up to 36% at pH 8.0, theoretical detection limits remained <100 pM, indicating that these DFB-based chips are robust enough to work across a wide pH range (Figure 4). These findings open the exciting possibility that similar biomimetic surfaces ultimately might be able to quantify the chemical speciation of iron in seawater; a goal now achieved only by time-intensive, laboratory-dependent voltammetric studies.

Regeneration of the Chips. To regenerate the iron-free DFB surface, the chips were rinsed with 5 mL of methanol to remove adsorbed organic matter, rinsed with 10 mL of 0.01 M HCl and deionized water, and soaked in 10 mM oxalic acid solution (pH 3.0) for 15 min to release iron from DFB through ligand exchange. After a final rinse with 5 mL of deionized water, the chips were dried with N_2. This regeneration procedure decreased the Fe−O peak at 560 cm^{-1} by more than 95% and the peaks from DOM by more than 96%. To determine whether repeated surface regeneration affected analytical sensitivity, three chips were exposed to seawater containing 0.5 nM Fe, analyzed by FT-IR, and the surface was regenerated. Repeating this cycle 10 times for each chip did not alter the measured iron concentration by more than 15% (Table 2).

Potential Interferences. Although DFB has low side reaction coefficients with the major salts in seawater,[5] some cations at high concentrations potentially could bind to unoccupied DFB sites and thereby interfere with iron analysis. To assess the potential for cation interferences, the chips were exposed to individual elemental solutions at or above seawater concentrations to identify peaks that might interfere with iron analysis at 560 cm^{-1} (Table 3). None of these cations interfered with iron determinations, and moreover, these peaks were not observed in the spectra of chips exposed to natural seawater (e.g., Figure 3C), likely due to side reactions with inorganic species or other metal-complexing organic ligands found for other metals in seawater.[46–49]

In addition to cations in the seawater matrix, sorption of iron-containing organic (or possibly inorganic) colloids to the DFB-modified surface presents another potential interference to the Fe−O bands at 560 cm^{-1}. We subjected silane-modified (but DFB-free) chips to natural seawater from a number of depths at Ocean Station PAPA. In no case did the IR spectra from these exposed substrates contain bands within the Fe−O peak integration limits (data not shown).

Recent studies show that Fe(II) can comprise a major fraction of total dissolved iron in surface waters during daylight.[12,50] Our experiments revealed that Fe(II) also reacts with immobilized DFB and is indistinguishable from Fe(III) in IR spectra. This result likely stems from rapid oxidation of Fe(II) by the DFB complex in the presence of dissolved oxygen; essentially, all of the iron complexed by DFB is Fe(III) at the time of analysis. In addition to facilitating Fe(II) oxidation in oxic waters, DFB also can oxidize Fe(II) under anoxic conditions,[50–51] a process that destroys the DFB ligand. Although we did not evaluate the chips under anoxic conditions, the inference is that use of DFB modified chips should be restricted to oxic seawaters.

Chip and Batch Uniformity. To determine chip reproducibility, 10 chips cut from different regions of the same wafer were analyzed spectroscopically. Each chip was saturated with Fe(III), and the integrated intensity of the Fe−O band at 560 cm^{-1} measured. Interchip variability was less than 4% among chips cut from the same wafer. This uniformity permits the use of a single series of calibration runs for all chips within the same batch.

It is difficult to precisely control polymerization of the trialkoxysilane (anhydride silane) with solution-phase synthesis because small differences in the amount of water on the silica surface significantly affect the degree of silane polymerization. While it

(46) Dupont, C. L.; Nelson, R. K.; Bashir, S.; Moffett, J. W.; Ahner, B. A. *Limnol. Oceanogr.* **2004**, *49*, 1754–1762.
(47) Moffett, J. W.; Brand, L. E. *Limnol. Oceanogr.* **1995**, *41*, 388–395.
(48) Saito, M. A.; Moffett, J. W. *Mar. Chem.* **2001**, *75*, 49–68.
(49) Ellwood, M. J. *Mar. Chem.* **2004**, *87*, 37–58.
(50) Farkas, E.; Enyedy, E. A.; Fabian, I. *Inorg. Chem. Commun.* **2003**, *6*, 131–134.
(51) Millero, F. J. *Chemical Oceanography*, 3rd ed.; CRC Taylor and Francis: New York, 2006.

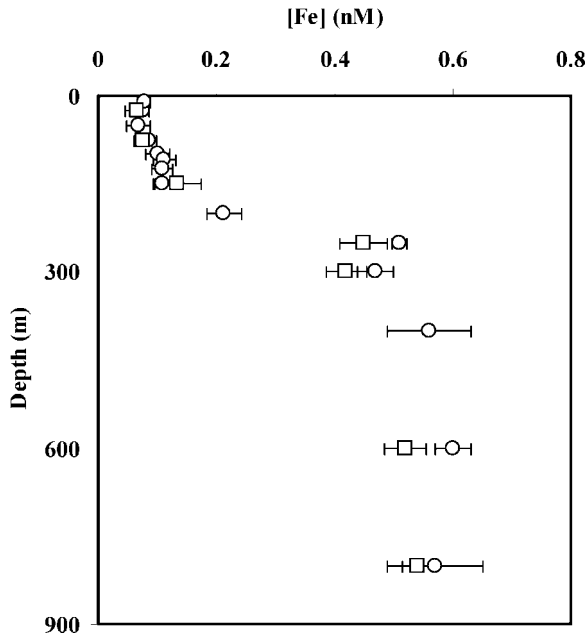

Figure 5. Depth profile of iron at Ocean Station PAPA (50°N 145°W) in May 2007. Iron was measured by shipboard analyses (FIA-CL) (open circles) and by DFB-modified chips (open squares). Shipboard FIA-CL data points represent the mean of triplicate measurements ±1 SD. The DFB chip-based data points represent the mean of duplicate measurements ± range.

is rather straightforward to control and eliminate water in vapor-phase silane attachment under vacuum, we found that vapor-phase treatment resulted in 99.5% fewer reactive carboxylic acid groups for DFB attachment than solution-phase synthesis and did not provide the needed IR sensitivity. Ideally, solution-phase synthesis would yield a single polysilane layer having all carboxylic acid groups reactive to amide coupling with DFB. In practice, the 3-D polymerization may leave up to 40% of the carboxylic acid groups buried in the polysilane matrix, causing the mass of DFB per chip to vary (0.10−0.24 mg) among batches. Even so, the moles of reactive DFB on each chip were in great excess over that of iron in 1 L of oceanic surface (<0.2 nM) and deep seawaters (~0.6 nM), and because 100% of the iron in solution becomes immobilized on the chip surface at pH 1.7, multiple calibrations are not necessary.

Field Samples. We tested the ability of this biomimetic sensing platform to provide accurate iron determinations at Ocean Station PAPA in the eastern subarctic Pacific, an iron-limited region where surface water (<100 m) iron concentrations are persistently among the lowest levels observed in any ocean waters. A depth profile for total iron measured by the DFB chips and by luminol chemiluminescence[43] is shown in Figure 5. These data show a classic nutrient-type depth distribution, consisting of a surface concentration minimum of ~80 pM Fe caused by iron uptake by phytoplankton in the photic zone. Iron concentrations increase with depth below the photic zone due to biological remineralization of sinking particulate matter. There is excellent agreement between the iron profile determined with our biomimetic, chip-based system and that obtained with the more conventional method of flow injection analysis with chemiluminescence detection.

CONCLUSION

This work has demonstrated that covalent immobilization of the siderophore desferrioxamine B to mesoporous silica films can be used to accurately and precisely measure ultratrace levels of iron in certified and natural seawater samples using FT-IR. The siderophore provides a high selectivity to the detection system by specifically concentrating iron on the mesoporous surface, with FT-IR analysis ensuring a second layer of analytical selectivity. Iron measurements were not complicated by other cations or by the sorption of marine dissolved organic matter. Although the DFB-modified film in principle has similarities to ligand-based solid-phase extraction, the ability to directly measure the Fe(III)−DFB complex on the chip greatly simplifies analyses by eliminating the need for wet chemistry-based, downstream detection systems. Unlike other reported iron sensors, this nanostructure-based detection system can measure total iron in acidified (pH < 1.8) samples, thereby enabling intercalibration with current methods[13] as well as direct comparisons with previously collected data. Moreover, iron recoveries to this device decrease with increasing pH as natural organic chelators in seawater increase their reactivity, suggesting that it may eventually be possible to probe the chemical speciation of iron in natural waters, and its relationship to iron availability to phytoplankton. Perhaps most importantly, the simplicity of the chip-based system offers scientists flexibility in sampling and analytical logistics. Iron can be measured on a field research platform using standard FT-IR instrumentation, or exposed chips can be returned to the laboratory in lieu of whole water samples. The findings here provide a critical step toward developing robust iron sensor technology for deployment on emerging ocean observing systems.

ACKNOWLEDGMENT

We thank the Captain and crew of the *R/V Thomas G. Thompson*. We also thank Morgan Brunbauer for assistance in the field and four anonymous reviewers for their valuable comments on the manuscript. This work was funded by NSF Grant BES-0304523, and additional student support was provided by NSF GK-12 (DGE-0231642) and IGERT SSEI (0504494) fellowships.

SUPPORTING INFORMATION AVAILABLE

Difference spectra for DFB-modified chips exposed to 1 L of seawater standard (pH 1.7) of 50, 100, and 300 pM Fe(III). For clarity, the spectrum of the corresponding 0 pM standard was used as a reference. Least-squares linear fits and R^2 values for figure. pH 1.7: $y = 0.0372x + 0.0007$, $R^2 = 0.9866$. pH 4.5: $y = 0.0321x + 0.0014$, $R^2 = 0.9836$. pH 8.0: $y = 0.0218x + 0.0013$, $R^2 = 0.9704$. This material is available free of charge via the Internet at http://pubs.acs.org.

Received for review February 20, 2008. Accepted April 3, 2008.

AC800356P